

Linear Dependence of Post-irradiation Input Bias Currents on Pre-irradiation Values in Silicon Bipolar Microcircuits

Yu Song,^{1,2,*} Jie Zhao,^{3,2} Shun Li,² Shi-Yao Hou,^{2,4} Hang Zhou,²
Yang Liu,² Ying Zhang,² Dechao Meng,² Gang Dai,² and Jian Zhang^{5,†}

¹College of Physics and Electronic Information Engineering, Neijiang Normal University, Neijiang 641112, China

²Microsystem and Terahertz Research Center & Institute of Electronic Engineering,
China Academy of Engineering Physics, Chengdu 610200, China

³Center for Circuits and Systems, Peng Cheng Laboratory, Shenzhen 518055, China

⁴College of Physics and Electronic Engineering & Center for Computational Sciences, Sichuan Normal University, Chengdu 610068, China

⁵School of Electronic Science and Engineering, University of Electronic Science and Technology of China, Chengdu 611731, China

(Dated: March 2, 2022)

We find in experiments a linear dependence of ionization irradiation-induced degradations on pre-irradiation values of the input bias current in bipolar devices with simple input stages. The dependence is found to generally exist in all studied cases of different device types and different irradiation conditions. A unique behavior of the energy distribution of the interface states (D_{it}) under irradiation is suggested as the origin of the observed phenomenon: the generation of interface traps through the depassivation of Si-H bonds located near the pre-irradiation interface traps displays a D_{it} as an enlarge of the initial D_{it} and results in the general linear dependence. A more accurate damage prediction method by using the pre-irradiation values is proposed based on the observed phenomenon.

I. INTRODUCTION

Linear bipolar microcircuits, such as operational amplifiers and voltage comparators, are widely used in space applications. Under persistent ionizing irradiations from the space, the electric properties of these devices will degrade, with the input bias current (IBC) usually as the most sensitive parameter. The variability of the total ionizing dose (TID) degradation of these devices is an important yet quite unexplored field. Manufacturer-to-manufacturer, lot-to-lot, wafer-to-wafer, part-to-part, and channel-to-channel response variabilities have been studied for several bipolar devices [1–15]. Large manufacturer variability was found for voltage comparators LM111, LM211, and LM311. The total dose degradation of the IBC varies by a factor of 100 among manufacturers, as the physical layout of these transistors is different for each vendor [2]. The response variability of 108A-type operational amplifier was compared at the diffusion lot, wafer, and sub-wafer levels for breakout transistors as well as complete circuits. It was found that the lower specification devices from the same wafer or diffusion lot could be used as test samples to determine the hardness of the low-yield 108A devices [4]. A strong part-to-part response variation is found in a voltage comparator LM111, for which the low doping of the substrate PNP input transistors was identified as the dominating mechanism [5]. Besides, an operational amplifier LM124 was found to exhibit a much weaker part-to-part response variation, which was attributed to the difference in the radiation-induced oxide defect build-up and circuit effects in this device [5]. Test of amplifiers LM124, LM111, and LM119, as well as comparators LM139 and LM193 from National Semiconductor reveals that the channel-to-channel vari-

ability was minor compared with the unit-to-unit or the wafer-to-wafer variation [6, 7]. The influence of dataset size and statistical model on the bounding estimates of TID degradation was examined and a method for selecting the model with greatest predictive power was developed [8]. Recently, inclusion of radiation environment variability in TID hardness assurance methodology has also been discussed [9, 10]. Besides, it is found that the lot-to-lot variability of amplifiers LM111, LM124, OP-27, OP-484, RH1014, and RH1056 can be altered by prior neutron irradiations on the samples [11].

Even for bipolar devices from the same manufacturer and a single lot, the variability of the degradation can stem from the variations of many factors due to the uncertainties in photo/etching, ion implantation, oxidation, passivation, packaging, and burn-in etc. These factors include the layer thickness [16], layer quality (concentration of oxygen vacancies) [17, 18], hydrogen concentration [19–21], and electric field [22, 23] in the base oxide, which determine the concentrations of oxide trapped charges (N_{ot}) and interface traps (N_{it}) generated from the irradiation. The factors also include the structure and doping parameters of the transistors [5, 24] as well as the operating point bias of the microcircuit [5, 25], which determine the contribution efficiency of the ionization defects to the base current and IBC. We notice that, the variations of these factors can also result in the variability of the pre-irradiation IBC. Hence, it is natural to ask if there is a clear dependence of the post-irradiation IBCs on the pre-irradiation values in the bipolar devices. However, to our best knowledge, there is barely such investigations.

In this work, we answer the question by carrying out systematic irradiation experiments on large-sample-size bipolar devices from the same manufacturer and the same lot. Three typical commercial off-the-shelf (COTS) bipolar devices with simple input stages are chosen as the research subjects. Remarkably, we find a general linear dependence of the irradiation response on the initial values of the IBC, which maintains for all investigated cases: three kinds of devices of differ-

* Corresponding author: kwungyusung@gmail.com

† Corresponding author: jianzhang@uestc.edu.cn

ent types and many irradiation conditions of different doses, dose rates, and temperatures. We attribute this general dependence to a unique response of the energy distribution of interface traps (D_{it}) under irradiation: the generation of interface traps near the initial ones results in the enlarge of D_{it} , which demonstrates as a linearly-dependent component in the post-irradiation IBC; the generation of interface traps away from the initial ones results in the overall shift of D_{it} , which displays as an independent component in the post-irradiation IBC. Based on the observed phenomenon, we examine the applicability of the traditional mean-value damage prediction method and propose a more accurate method for bipolar devices whose post-irradiation IBCs display strong dependence on the pre-irradiation values.

II. EXPERIMENTAL SETUP

To investigate the variability of the irradiation-induced degradation in bipolar devices, one quad comparators, LM2901, and two quad-operational amplifiers, MC4741 and LM324N, are used in our experiments. These devices are chosen due to three reasons. First, bipolar devices with simple input stages are chosen to avoid nonlinearity of TID response in devices with compensated input stages [26–28]. The circuit schematic of LM2901 [29] is shown in Fig. 1, from which a simple input stage can be seen. Secondly, both comparators (LM2901) and amplifiers (MC4741 and LM324N) are chosen for generality. Thirdly, both amplifiers with NPN-type (MC4741) and PNP-type (LM324N) input stages are chosen for generality. For clearness, the characteristics of these devices and the related test conditions are summarized in Tables I and II, respectively.

TABLE I. Characteristics of the devices.

Type	Manufacture	Function	Input stage	Package
LM2901	TI	Quad comparator	PNP	PDIP (14)
MC4741	Motorola	Quad op amp	NPN	Plastic DIP
LM324N	TI	Quad op amp	PNP	PDIP (14)

TABLE II. Test conditions of the devices.

Type	Test size	Dose rate	Temperature
LM2901	75×4	0.1 rad/s	25°C
	25×4	100 rad/s	25°C
MC4741	75×4	0.1 rad/s	25°C
	25×4	100 rad/s	25°C
LM324N	6×4	10 rad/s	25°C
	4×4	10 rad/s	80°C
	4×4	10 rad/s	120°C
	4×4	10 rad/s	175°C

The experiments are carried out according to the standard test procedure, MIL-STD-883-G, Test Method 1019.7. For each type of device, large sample sizes are used to obtain credible results. For LM2901 and MC4741, 25×4 (75×4) devices were chosen randomly from the same manufacturer and a same lot and irradiated with high (low) dose rate. For

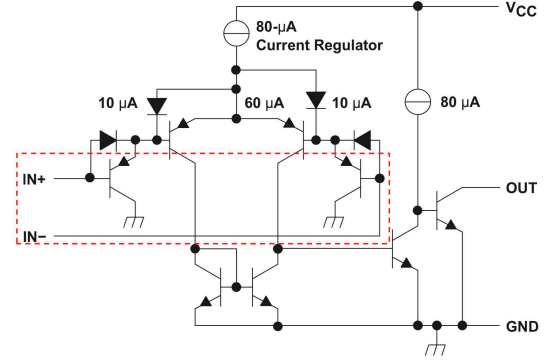


FIG. 1. (color online) Circuit schematic of quad comparators LM2901 [29].

LM324N, 6×4 (4×4) devices were randomly chosen from the same manufacturer and a single lot and irradiated at room (higher) temperature. Every single device was labelled so that its parameter changes can be tracked.

The radiation source is a Cobalt-60 gamma ray source in Xinjiang Technical Institute of Physics & Chemistry, Chinese Academy of Sciences. Dosimetry was performed using an ionizing radiation absorption dose measurement system containing a PTW 0.6cc Farmer ionization chamber. The expanded uncertainty of the measurement is 4.052% and the confidence coefficient is 95%.

In order to irradiate multiple devices at the same time while ensuring identical levels of dose rate on each device, all 75×4 or 25×4 (6×4 or 4×4) devices were closely placed on an irradiation board so as to lie on the same isodose panels. The irradiation board measures 30cm × 30cm and the total dose difference at any point on it is no more than 5% for all the chosen radiation dose rates. The chips are irradiated with all pins grounded.

To consider the possible influence of irradiation dose, dose rate, and temperature on the variability of the TID effects, the devices LM2901 and MC4741 are irradiated at high dose rate (100 rad/s(Si)) and low dose rate (0.1 rad/s(Si)) field at room temperature, while the devices LM324N are irradiated at room temperature and high temperature ($T = 80, 120, \text{ and } 175^\circ\text{C}$) at 10 rad/s(Si) dose rate, respectively; see Tab. II. The elevated temperature is provided by an ESPEC heating system with accuracy of $\pm 2^\circ\text{C}$. For LM2901 and MC4741, parameters are measured when the total dose is accumulated to 10 krad (Si), 30 krad (Si), 50 krad (Si), and 100 krad (Si). For LM324N, the total dose is accumulated to 5 krad, 10 krad, 30 krad, 50 krad, and 100 krad.

Electrical parameters of the devices were measured at room temperature for pre- and post-irradiation. For the quad comparator LM2901N, we tracked the following parameters: input offset voltage (V_{io}), IBC ($I_b, +/ -$), input offset current (I_{io}), open loop gain in dB (A_{vd}), and output voltage (V_o). For the quad operational amplifiers MC4741 and LM324N, we measured the following parameters: V_{io} , $I_b (+/ -)$, I_{io} , A_{vd} , and common-mode rejection ratio (K_{cmr}). Remote testing were performed with an integrated parameter analyzer for ampli-

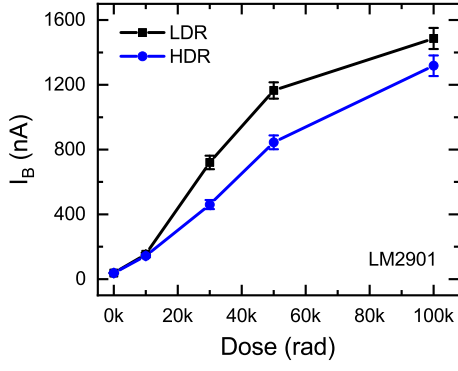


FIG. 2. (color online) The average value and standard deviation of IBCs of comparator LM2901 as functions of the total dose. Black (blue) for 75×4 (25×4) comparators irradiated at low (high) dose rate.

fiers and comparator, SIMI3193. The analyzer provides a test box and a test adapter to minimize the impact of leakage on the measurements. The analyzer has a current resolution down to 0.1nA and an uncertainty less than 5%. The resolution is much smaller than the smallest pre-irradiation IBC (~ 10 nA). Each test was finished within half an hour after irradiation to guarantee that the annealing process does not have a great impact on the result.

III. RESULTS AND DISCUSSION

Our results show that, for all three types of device, the IBC is the most sensitive parameter. So, we focus on the variability of this parameter here. The pre- and post-irradiation IBC are denoted by I_B^0 and I_B , respectively. $\Delta I_B = I_B - I_B^0$ is the γ -ray induced ionization damage.

A. Linear I_B^0 dependence in comparator LM2901

The changes in the IBC of comparator LM2901 as function of the total dose are shown in Fig. 2. We can see clearly that the mean value of I_B increases monotonically as the total dose increases. For each tested dose, the observed IBC at low dose rate are always larger than that of the high dose rate, indicating the presence of an enhanced low-dose-rate sensitivity (ELDRS) effect [30] for LM2901. We also observe that as the total dose increases, the current-dose curves of these samples do not crossover; instead, the differences of I_B between samples increase with increasing dose, which leads to a *spread* behavior of the data; see the increasing standard deviations (error bars) in Fig. 2. This behavior was also observed in the input offset voltage of operational amplifiers LM324 and LM358 [31].

Does this interesting behavior imply a deep relation between the post-irradiation IBC and the pre-irradiation ones? To testify this speculation, in Fig. 3 we make a post-irradiation vs. pre-irradiation (P-P) plot to describe the damage of all tested samples. Remarkably, it is seen that, the whole trend

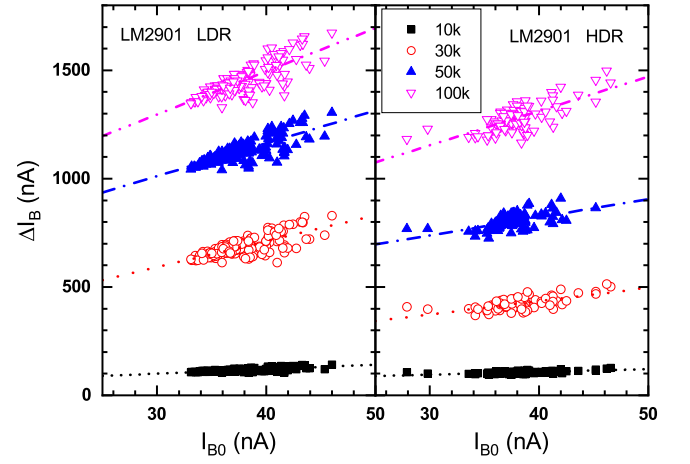


FIG. 3. (color online) IBC's degradations versus the pre-irradiation values for comparator LM2901 irradiated at low (left panel) and high (right panel) dose rate. The short-dashed, dotted, dash-dotted, and dash-dot-dotted lines represent the linear fitting of the data at different total doses as indicated in the figure.

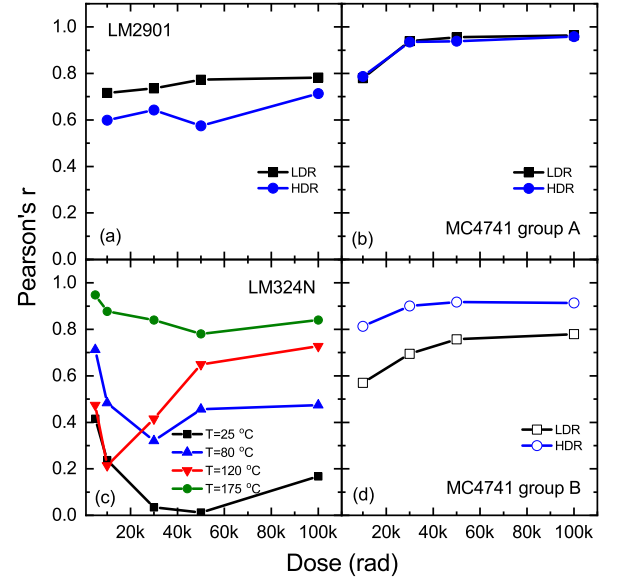


FIG. 4. (color online) Pearson's correlation coefficients for the linear dependence as a function of total dose for LM2901 (a), group A of MC4741 (b), group B of MC4741 (d), and LM324N (c).

of the damage follows a simple linear dependence on the pre-irradiation values. In other words, the samples with larger pre-irradiation IBCs will degrade more. Moreover, from the figure, the linear dependence maintains for any dose and for both the low and high dose rates. To further confirm the dependence, the Pearson's correlation coefficient is calculated and plotted in Fig. 4 (a). From the results, we can confirm a linear dependence of the irradiation response on the initial value of IBC; moreover, it is seen that the higher the irradiation dose, the more significant the linear dependence.

The $\Delta I_B - I_B^0$ data can be fitted using a linear regression

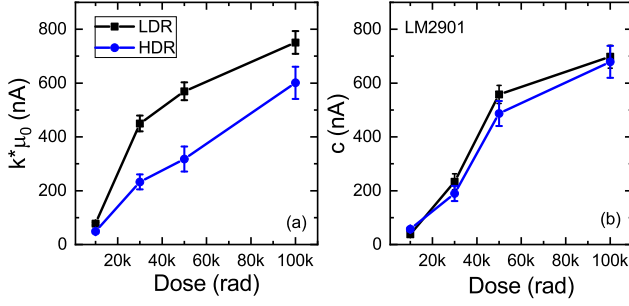


FIG. 5. (color online) The linearly-dependent component $k \times \mu_0$ (a) and the independent component c (b) as functions of the total dose for comparator LM2901. Black (blue) for low (high) dose rate.

model:

$$\Delta I_B(I_B^0) = k \times I_B^0 + c, \quad (1)$$

where k is the slope of the linear dependence and c is a constant component independent of the pre-irradiation IBC. The linearly-dependent component of ΔI_B then can be calculated as $k \times \mu_0$, where μ_0 is the mean value of I_B^0 . The results are plotted in Fig. 5, from which we obtain that both the linear and constant component increase for increasing dose at a fixed dose rate and both increase for decreasing dose rate at a fixed dose that is larger than 10 krad (Si).

B. Linear I_B^0 dependence and bimodal response in OA MC4741

One may wonder whether the observed linear dependence be specific for the investigated device. To this end, we investigate another bipolar device, operational amplifier MC4741. Its input stage is also simple but the input transistor is NPN

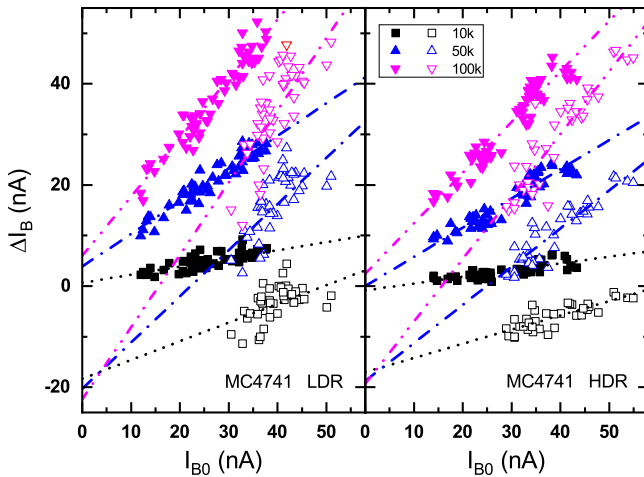


FIG. 6. (color online) Degradations of IBC versus the pre-irradiation IBC for amplifier MC4741 irradiated at low (left panel) and high (right panel) dose rate. The data are divided into two groups due to their different responses. The lines represent the linear fitting of the data at different total dose as indicated in the figure.

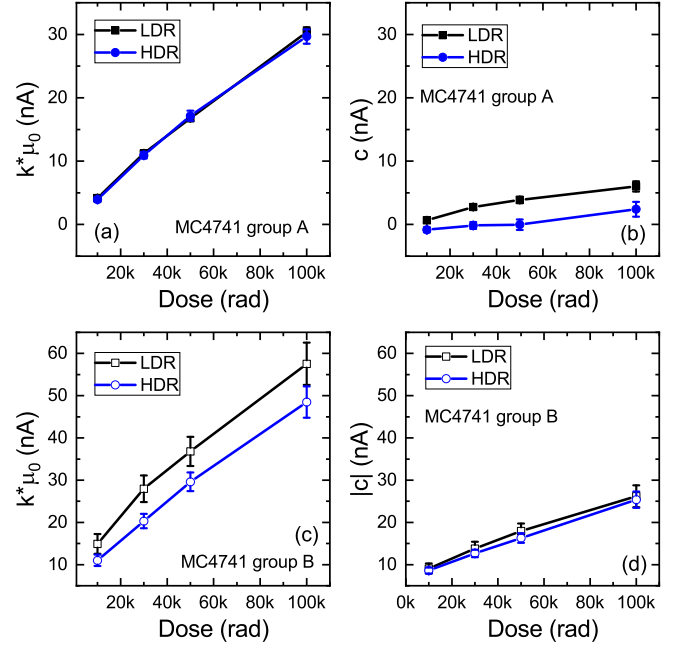


FIG. 7. (color online) The linearly-dependent component $k \times \mu_0$ (a, c) and the independent component c (b, d) as functions of the total dose for amplifier MC4741. The solid (open) symbols represent the data for group A (B) as explained in the caption of Fig. 6. Note, in (d) the current is negative and plotted in its absolute value.

type. The P-P plot is present in Fig. 6. A linear I_B^0 dependence is also observed for ΔI_B of this device. Actually, the Pearson's correlation coefficients (see Fig. 4 (b)) is even larger than those for LM2901. Similar to LM2901, the linear dependence becomes more significant for increasing dose. The linearly-dependent and independent components are extracted using Eq. (1) and plotted in Fig. 7 (a) and (b). It is seen that, while the two components are comparable for LM2901, here the dependent current is much larger than the independent current in MC4741.

From Fig. 6, we have another important observation: the irradiation response of MC4741 is bimodal. The bimodal response is that, for any doses, there is a group (group B) which has the similar slopes as the normal group (group A) but negative intercepts, see Fig. 7 (c) and (d), respectively. For the Pearson's correlation coefficients, see Fig. 4 (d). The bimodal response was also observed in the IBC of LM111 [32] and the input offset voltage of LM358 [31]. To investigate the possible reason, we plot the current-dose profile for each group in Fig. 8. For group A, we see clearly a spread behavior of the damage similar to Fig. 2: the larger the dose the bigger the standard deviations. For group B, besides the spread behavior, the average value of IBCs first decreases and then increases with the increasing gamma ray dose. As the input offset voltage in LM358 is a complex function of the total dose for each type of the input stage, the authors of Ref. [31] connected the bimodal behavior of it to the "circuit" factor, i.e., the asymmetry of a current mirror of the differential stage as well as the difference of I-V characteristics of differential pair transistors. Here, the IBC of the devices are directly related to the base

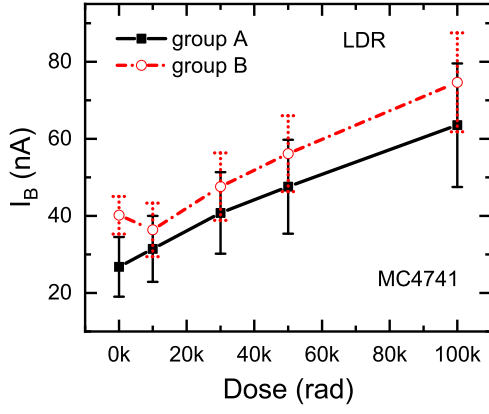


FIG. 8. (color online) The average value and standard deviation of IBCs as functions of the total dose for amplifier MC4741, irradiated with low dose rate. Black (red) for amplifiers from the group A (B).

current of the input-stage transistors [3, 25, 27, 32]. On the other hand, from Fig. 8 we notice that, the devices of group B have a larger initial IBCs than those of devices of group A. So, there should be pre-existing defects in silicon of group B devices due to the process of ion implantation, and the abnormal decrease behavior of IBCs of group B devices is an annealing of these defects under ionization irradiation. Such an annealing is the so-called injection annealing [33], in which the re-ordering of pre-existing defects is enhanced by the presence of free charge carriers induced by ionization irradiation, due to the change in defect charge states and enhancement of defect mobility [14, 15, 34]. Nevertheless, although the MC4741 device response in a bimodal way, the post-irradiation IBCs still linearly depend on the pre-irradiation ones.

C. Linear I_B^0 dependence in LM324N at high temperature

The experiments for comparator LM2901 and amplifier MC4741 are performed at room temperature. Would the linear dependence hold for high-temperature irradiation? To check this possibility, we performed the gamma ray irradiation experiments for amplifier LM324N (with PNP-type simple input stage) at both room temperature ($T = 25^\circ\text{C}$) and high temperatures of $T = 80, 120$, and 175°C . The dose rate is set to 10 rad(Si)/s . The P-P plot of obtained results are shown in Fig. 9. It is seen that the linear I_B^0 dependence of ΔI_B also holds for these higher temperatures. This is clearly reflected by the Pearson's correlation coefficient, which is plotted in Fig. 4 (c) as a function of the total dose for different temperatures. Different from the other two devices, the coefficient first decreases and then increases with increasing dose. On the other hand, the higher the temperature, the more significant the linear dependence.

The two derived current components using Eq. (1) are displayed in Fig. 10. It is seen that the linearly-dependent current component is much sensitive to the elevated temperature than the independent current component. At room temperature, the independent current component dominates; at higher temper-

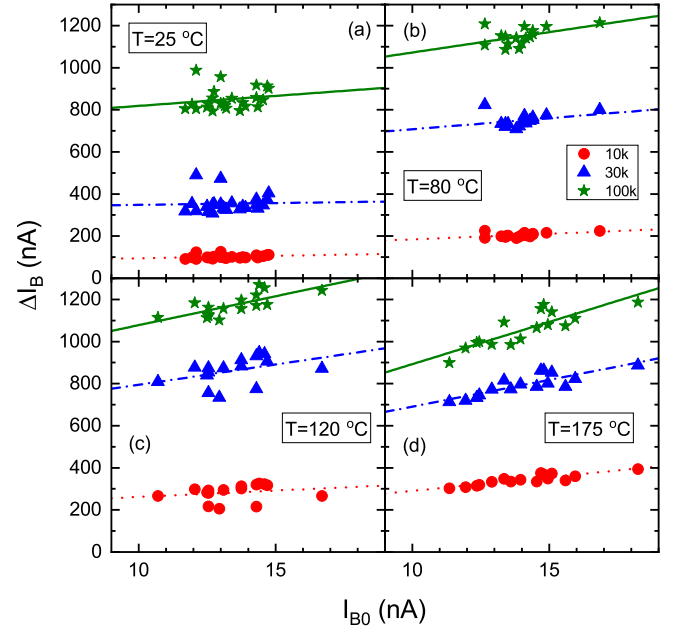


FIG. 9. (color online) Degradations of the IBC versus the pre-irradiation IBC for amplifiers LM324N. The lines represent the linear fitting of the data at different total dose as indicated in the figure. The experiments are performed at room temperature $T = 25^\circ\text{C}$ (a) and at high temperatures with $T = 80^\circ\text{C}$ (b), 120°C (c), and 175°C (d), respectively.

ature, the dependent current component becomes comparable or even larger.

D. Possible Mechanism of the observed linear dependence

The linear dependence of ΔI_B on I_{B0} is observed in devices of different manufacturers, different structures, and different irradiation conditions (see Tabs. I and II). These facts suggest that the linear dependence is a rather general phenomenon that is independent to the specific process and structure of the device. In following, we will suggest that such a general phenomenon may stem from a unique behavior of the energy distribution of the interface states (D_{it}) under ionization irradiation.

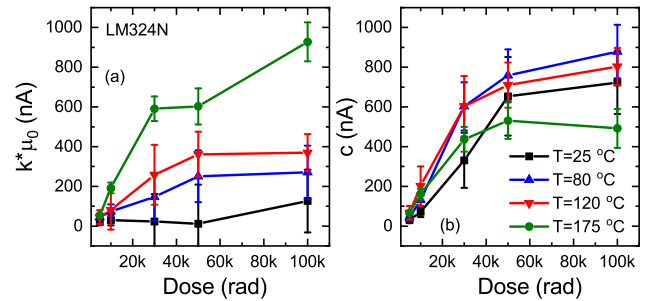


FIG. 10. (color online) The linearly-dependent component $k \times \mu_0$ (a) and the independent component c (b) as functions of the total dose for amplifier LM324N.

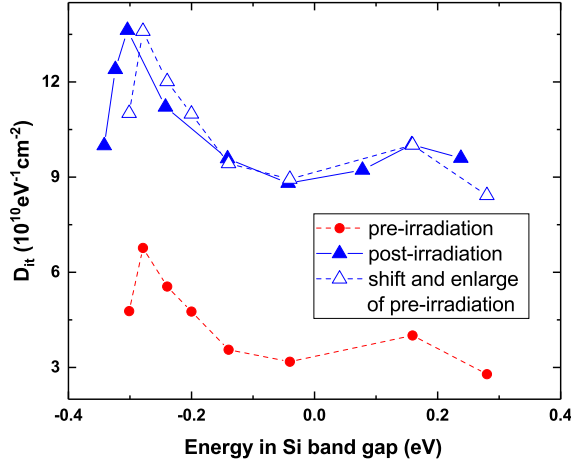


FIG. 11. (color online) The interface state distribution in the energy gap of Si before (red dashed) and after (blue dashed) ionization irradiation. As shown by the blue solid curve, the latter is found to be an overall shift and enlarge of the former, $D_{it}(E) = 1.3 \times D_{it}^0(E) + 4.8$. The data are adopted from Ref. [35].

tion. There are three reasons. Firstly, it is noticed that the linear dependence are observed even at very small total dose. As indicated in Refs. [3, 25, 27, 32], in this situation the IBC of the devices are directly related to the base current of the input-stage transistors. Secondly, the base current is determined by the surface recombination velocity, which is a product of the capture cross-section and the density of interface states in the oxide above the base region [36]. The capture cross-section is almost unchanged under irradiation, hence, the irradiation-induced change in D_{it} can dominate the origin of the linear dependence between ΔI_B and I_{B0} . Thirdly and lastly, we do find a linear dependence of the post-irradiation interface state distribution on the pre-irradiation one, see below for details.

As observed in experiments [35, 37], the pre-irradiation interface state distributes nonuniformly in the energy gap of silicon, see the red dots in Fig. 11. Due to the variability of the structure parameters of the base region, the input-stage transistors of the same manufacturer and a single lot can have different effective Fermi levels in the base, at which the densities of interface state are different. This leads to different interface recombination velocities, hence different base currents of the transistors and different IBCs of the devices.

Under ionization irradiation, new interface traps will be generated due to the depassivation of Si-H bonds by protons at the interface [38, 39], see the blue dots in Fig. 11. The protons are released in the bulk silica through the interaction of irradiation-induced oxide trapped charges and hydrogen [40]. Interestingly, the generated interface state displays a similar distribution as the pre-irradiation D_{it} [35, 37], see Fig. 11. The reason is that, a part of the Si-H bonds is located near the initial interface traps and has a similar physical environment [35]. Hence, at any fixed energy, the larger the initial D_{it} , the larger the generated D_{it} under certain irradiation dose. As a result, devices with larger IBCs, i.e., with larger interface states near their Fermi energies, will have larger increase of interface states after certain irradiation, hence have larger

increase of IBCs. This is the observed linear I_B^0 dependence of the ΔI_B .

The irradiation-induced D_{it} was believed to be proportional to the pre-irradiation D_{it} [35, 37]. However, our calculation shows that the change is actually an overall shift plus an enlarge of the initial distribution, see the dashed curve in Fig. 11, which shows a higher position and an enhanced peak-to-valley ratio relative to the initial distribution profile. The overall shift happens because the other part of Si-H bonds is far away from the initial interface traps, and the generated interface states should display an uniform energy distribution that has no relation with the initial D_{it} . The total change of D_{it} induced by irradiation can be expressed as

$$\Delta D_{it}(E) = k' \times D_{it}^0(E) + c'. \quad (2)$$

As the initial and generated D_{it} near the Fermi energy corresponds to the pre-irradiation and post-irradiation IBC, respectively, a linear dependence of the same form should be observed for the IBC of the devices. This is just Eq. (1) and the results as obtained in Figs. 3, 6, and 9. It is noticed that, the irradiation-induced enlarge of the D_{it} is indispensable for the linearly-dependent component in Eq. (1), while the irradiation-induced overall shift of the D_{it} is response for the independent component in Eq. (1). As the dose increases, both the enlarge and shift of the D_{it} increases. This corresponds to the dose dependence of the linearly-dependent and independent components observed in Figs. 5, 7, and 10.

As mentioned above, the linear component is dominant in MC4741, while the constant component becomes dominant in LM324N. These results can be explained self-consistently based on the above picture. In MC4741, it is seen that the irradiation-induced increase of IBC is comparable with the initial value of IBC. This fact implies that most of the interface traps are generated through the Si-H bonds around the initial interface traps. As a result, the enlarge of D_{it} dominates the irradiation response and one observes a dominating linear component in the IBC of this device. In LM324N, the irradiation-induced increase of IBC is much larger than the initial value of it. This fact reflects that plenty interface traps are generated away from the initial ones. So, the shift of the D_{it} dominates the response process and a larger independent component is observed in the IBC of this device.

E. Damage Prediction Using the Dependence Phenomenon

In practice, the irradiation degradations of the IBC of to-be-use devices are usually estimated by the mean damage of randomly selected samples from the same lot. Here, we indicated that, this method can be inapplicable when the linearly-dependent component is comparable with or even larger than the independent component (e.g., the LM2901 and MC4741 cases). This is because, in these cases samples with small difference in I_B^0 (several nA) can response very differently to the same irradiation (hundreds of nA), see Figs. 3 and 6. As a result, the damages can be very different for each sample to be used and each sample has been tested. For example, in the case of MC4741, the maximal damage can be 2.5 times of

the minimal damage. Here, based on the observed linear dependence, we propose that the damages of to-be-used samples can be more precisely predicted by using their pre-irradiation IBCs as an index. Specifically, using Eq. (1), the damages can be predicted by the pre-irradiation currents times the slope and plus the intercept; the slope and the intercept can be obtained by carrying out large-size sample irradiation experiment and extracting parameters from the P-P plot of the data. It should be indicated that the proposed method also become inapplicable for devices displaying bimodal response. Of course, when the independent component dominates (the LM324N case), the traditional prediction method can be used to estimate the damages.

IV. CONCLUSION

In summary, we have found a general experimental phenomenon in the irradiation response of COTS bipolar devices with simple input stages. It is demonstrated that for devices from the same manufacturer and the same lot, samples with larger pre-irradiation IBCs will statistically degrade more under the same irradiation. This linear dependence widely exists in all investigated cases, despite of the huge discrepancy in the device types, bimodal response, and irradiation conditions (dose, dose rate, and temperature). We indicate that such a general phenomenon may stem from the unique behavior of the energy distribution of the interface states under irradiation. The overall shift of the pre-irradiation D_{it} , which is due

to the generation of interface traps away from the initial ones, is indispensable for the independent component of the post-irradiation IBC. The enlarge of the pre-irradiation D_{it} , which stems from the generation of interface traps located near the initial ones, is responsible for the linearly-dependent component of the post-irradiation IBC. Due to this mechanism, the linear I_B^0 -dependence can be expected in other bipolar devices with simple input stages. Our results also show that, the irradiation-induced linearly-dependent current can be comparable with the independent current in some bipolar devices. In this case, the traditional average-value damage prediction method can be inapplicable. Instead, we propose that the damage of to-be-use devices can be more precisely predicted by using the observed dependence phenomenon and the pre-irradiation currents.

ACKNOWLEDGMENTS

We owe to an anonymous reviewer, without whose suggestions we will not connect the observed linear dependence with the energy distribution of the interface states. We also thank Dr. B.S. Tolleson of the Arizona State University and Prof. D.M. Fleetwood of the Vanderbilt University for insightful suggestions. This work was supported by the Science Challenge Project (Grant No. TZ2016003-1) and National Natural Science Foundation of China (Grant Nos. 11804313 and 11404300).

-
- [1] R. R. Blair, Surface effects of radiation on transistors, IEEE Trans. Nucl. Sci. 10 (5) (1963) 35–44.
 - [2] J. Krieg, T. Tuflinger, R. Pease, Manufacturer variability of enhanced low dose rate sensitivity (eldrs) in a voltage comparator, in: 2001 IEEE Radiation Effects Data Workshop. NSREC 2001. Workshop Record. Held in conjunction with IEEE Nuclear and Space Radiation Effects Conference (Cat. No.01TH8588), 2001, pp. 167–171.
 - [3] R. L. Pease, W. E. Combs, A. Johnston, T. Carriere, C. Poivey, A. Gach, S. McClure, A compendium of recent total dose data on bipolar linear microcircuits, in: 1996 IEEE Radiation Effects Data Workshop, 1996, pp. 28–37.
 - [4] A. H. Johnston, C. A. Lancaster, A total dose homogeneity study of the 108a operational amplifier, IEEE Trans. Nucl. Sci. 26 (6) (1979) 4769–4774.
 - [5] H. J. Barnaby, C. R. Cirba, R. D. Schrimpf, D. M. Fleetwood, R. L. Pease, M. R. Shaneyfelt, T. Tuflinger, J. F. Krieg, M. C. Maher, Origins of total-dose response variability in linear bipolar microcircuits, IEEE Trans. Nucl. Sci. 47 (6) (2000) 2342–2349.
 - [6] K. Kruckmeyer, L. McGee, B. Brown, D. Hughart, Low dose rate test results of national semiconductor’s eldrs-free bipolar amplifier lm124 and comparators lm139 and lm193, in: 2008 IEEE Radiation Effects Data Workshop, 2008, pp. 110–117.
 - [7] K. Kruckmeyer, L. McGee, B. Brown, L. Miller, Low dose rate test results of national semiconductor’s eldrs-free bipolar comparators lm111 and lm119, in: 2009 European Conference on Radiation and Its Effects on Components and Systems, 2009, pp. 586–592.
 - [8] R. Ladbury, J. L. Gorelick, S. S. McClure, Statistical model selection for tid hardness assurance, IEEE Trans. Nucl. Sci. 56 (6) (2009) 3354–3360.
 - [9] M. A. Xapsos, C. Stauffer, A. Phan, S. S. McClure, R. L. Ladbury, J. A. Pellish, M. J. Campola, K. A. LaBel, Inclusion of radiation environment variability in total dose hardness assurance methodology, IEEE Trans. Nucl. Sci. 64 (1) (2017) 325–331.
 - [10] I. V. Elushov, G. I. Zebrev, Taking into account the space environments variability for prediction of dose response in bipolar devices, IOP Conf. Ser.: Mater. Sci. Eng. 151 (1) (2016) 012002.
 - [11] J. L. Gorelick, R. Ladbury, L. Kanchawa, The effects of neutron irradiation on gamma sensitivity of linear integrated circuits, IEEE Transactions on Nuclear Science 51 (6) (2004) 3679–3685.
 - [12] J. Guillermin, N. Sukhaseum, A. Varotsou, A. Privat, P. Garcia, M. Vaillé, J. C. Thomas, N. Chatry, C. Poivey, Part-to-part and lot-to-lot variability study of tid effects in bipolar linear devices, in: 2016 16th European Conference on Radiation and Its Effects on Components and Systems (RADECS), 2016, pp. 1–8.
 - [13] A. N. Bozovich, F. Irom, Compendium of single event transient (set) and total ionizing dose (tid) test results for commonly used voltage comparators, in: 2017 IEEE Radiation Effects Data Workshop (REDW), 2017, pp. 1–21.
 - [14] Y. Song, H. Zhou, X.-F. Cai, Y. Liu, P. Yang, G.-H. Zhang, Y. Zhang, M. Lan, S.-H. Wei, Defect dynamics model of synergistic effect in neutron-and gamma-ray-irradiated silicon npn

- transistors, *ACS Applied Materials & Interfaces* 12 (26) (2020) 29993–29998.
- [15] Y. Song, S.-H. Wei, Origin of irradiation synergistic effects in silicon bipolar transistors, *ACS Applied Electronic Materials* 2 (12) (2020) 3783–3793.
- [16] D. M. Fleetwood, T. L. Meisenheimer, J. H. Scofield, 1/f noise and radiation effects in mos devices, *IEEE Trans. Electron Devices* 41 (11) (1994) 1953–1964.
- [17] J. Boch, F. Saigné, A. Touboul, S. Ducret, J.-F. Carlotti, M. Bernard, R. Schrimpf, F. Wrobel, G. Sarraeyrouse, Dose rate effects in bipolar oxides: Competition between trap filling and recombination, *Applied physics letters* 88 (23) (2006) 232113.
- [18] J. Boch, F. Saigné, L. Dusseau, R. Schrimpf, Temperature effect on geminate recombination, *Applied physics letters* 89 (4) (2006) 042108.
- [19] R. L. Pease, P. C. Adell, B. G. Rax, X. J. Chen, H. J. Barnaby, K. E. Holbert, H. P. Hjalmarson, The effects of hydrogen on the enhanced low dose rate sensitivity (eldrs) of bipolar linear circuits, *IEEE Transactions on Nuclear Science* 55 (6) (2008) 3169–3173.
- [20] P. C. Adell, R. L. Pease, H. J. Barnaby, B. Rax, X. J. Chen, S. S. McClure, Irradiation with molecular hydrogen as an accelerated total dose hardness assurance test method for bipolar linear circuits, *IEEE Transactions on Nuclear Science* 56 (6) (2009) 3326–3333.
- [21] D. M. Fleetwood, Effects of hydrogen transport and reactions on microelectronics radiation response and reliability, *Microelectronics Reliability* 42 (4) (2002) 523–541.
- [22] D. Fleetwood, S. Kosier, R. Nowlin, R. Schrimpf, R. Reber, M. DeLaus, P. Winokur, A. Wei, W. Combs, R. Pease, Physical mechanisms contributing to enhanced bipolar gain degradation at low dose rates, *IEEE Transactions on Nuclear Science* 41 (6) (1994) 1871–1883.
- [23] D. Fleetwood, L. Riewe, J. Schwank, S. Witczak, R. Schrimpf, Radiation effects at low electric fields in thermal, simox, and bipolar-base oxides, *IEEE Transactions on Nuclear Science* 43 (6) (1996) 2537–2546.
- [24] A. Wu, R. D. Schrimpf, H. J. Barnaby, D. M. Fleetwood, R. L. Pease, S. L. Kosier, Radiation-induced gain degradation in lateral pnp bjts with lightly and heavily doped emitters, *IEEE Trans. Nucl. Sci.* 44 (6) (1997) 1914–1921.
- [25] H. J. Barnaby, R. D. Schrimpf, R. L. Pease, P. Cole, T. Turflinger, J. Krieg, J. Titus, D. Emily, M. Gehlhausen, S. C. Witczak, M. C. Maher, D. van Nort, Identification of degradation mechanisms in a bipolar linear voltage comparator through correlation of transistor and circuit response, *IEEE Trans. Nucl. Sci.* 46 (6) (1999) 1666–1673.
- [26] H. Barnaby, H. Tausch, R. Turfler, P. Cole, P. Baker, R. Pease, Analysis of bipolar linear circuit response mechanisms for high and low dose rate total dose irradiations, *IEEE Transactions on Nuclear Science* 43 (6) (1996) 3040–3048.
- [27] L. Dusseau, M. Bernard, J. Boch, J.-R. Vaillé, F. Saigné, R. Schrimpf, E. Lorfèvre, J. David, Analysis of total-dose response of a bipolar voltage comparator combining radiation experiments and design data, *IEEE transactions on nuclear science* 53 (4) (2006) 1910–1916.
- [28] A. H. Johnston, B. G. Rax, Testing and qualifying linear integrated circuits for radiation degradation in space, *IEEE Trans. Nucl. Sci.* 53 (4) (2006) 1779–1786.
- [29] LM339, LM239, LM139, LM2901 Quad Differential Comparators datasheet.
URL <http://www.ti.com.cn/product/cn/LM2901/technicaldocuments>
- [30] E. W. Enlow, R. L. Pease, W. Combs, R. D. Schrimpf, R. N. Nowlin, Response of advanced bipolar processes to ionizing radiation, *IEEE Trans. Nucl. Sci.* 38 (6) (1991) 1342–1351.
- [31] A. Bakerenkov, V. Pershenkov, V. Felitsyn, A. Rodin, V. Telets, V. Belyakov, A. Zhukov, N. Gluhov, Experimental estimation of input offset voltage radiation degradation rate in bipolar operational amplifiers, in: 2019 IEEE 31st International Conference on Microelectronics (MIEL), IEEE, 2019, pp. 251–254.
- [32] J. Krieg, T. Turflinger, J. Titus, P. Cole, P. Baker, M. Gehlhausen, D. Emily, L. Yang, R. L. Pease, H. Barnaby, R. Schrimpf, M. C. Maher, Hardness assurance implications of bimodal total dose response in a bipolar linear voltage comparator, *IEEE Trans. Nucl. Sci.* 46 (6) (1999) 1627–1632.
- [33] B. Gregory, Injection-stimulated vacancy reordering in p-type silicon at 76° k, *Journal of Applied Physics* 36 (12) (1965) 3765–3769.
- [34] L. Kimerling, Recombination enhanced defect reactions, *Solid-State Electronics* 21 (11-12) (1978) 1391–1401.
- [35] T. Ma, G. Scoggan, R. Leone, Comparison of interface-state generation by 25-keV electron beam irradiation in p-type and n-type mos capacitors, *Applied Physics Letters* 27 (2) (1975) 61–63.
- [36] R. F. Pierret, G. W. Neudeck, *Advanced semiconductor fundamentals*, Vol. 6, Addison-Wesley Reading, MA, 1987.
- [37] L. Sivo, H. Hughes, E. King, Investigation of radiation-induced interface states utilizing gated-bipolar and mos structures, *IEEE Transactions on Nuclear Science* 19 (6) (1972) 313–319.
- [38] N. Saks, D. Brown, Interface trap formation via the two-stage h/sup+/process, *IEEE Transactions on Nuclear Science* 36 (6) (1989) 1848–1857.
- [39] S. N. Rashkeev, D. M. Fleetwood, R. D. Schrimpf, S. T. Pantelides, Defect generation by hydrogen at the si- sio₂ interface, *Phys. Rev. Lett.* 87 (16) (2001) 165506.
- [40] R. Stahlbush, B. Mrstik, R. Lawrence, Post-irradiation behavior of the interface state density and the trapped positive charge, *IEEE Transactions on Nuclear Science* 37 (6) (1990) 1641–1649.